Science Advances
AAAS

Supplementary Materials for

AFF3, a susceptibility factor for autoimmune diseases, is a molecular facilitator of immunoglobulin class switch recombination

Shin-ichi Tsukumo *et al.*

Corresponding author: Koji Yasutomo, yasutomo@tokushima-u.ac.jp

Sci. Adv. **8**, eabq0008 (2022)
DOI: 10.1126/sciadv.abq0008

This PDF file includes:

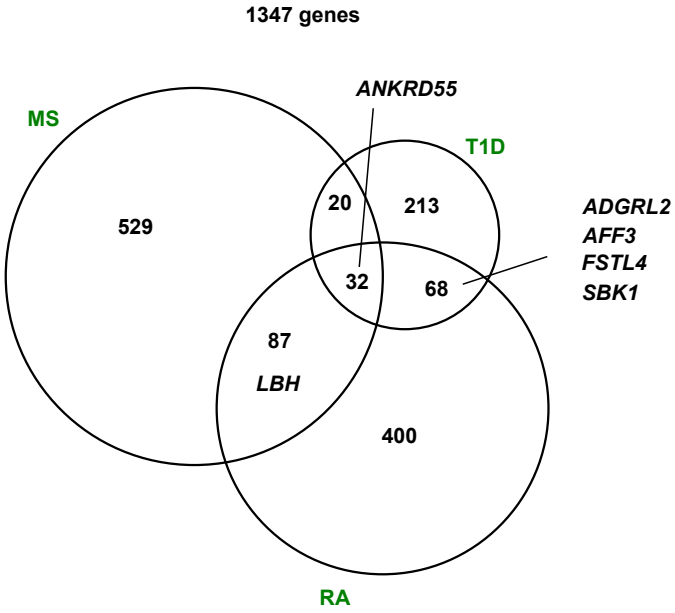
1347 genes
ANKRD55
MS
T1D
529
20
213
ADGRL2
AFF3
FSTL4
SBK1
32
68
87
LBH
400
RA

Fig. S1. Venn diagram of genes potentially related to rheumatoid arthritis (RA), multiple sclerosis (MS), and type 1 diabetes (T1D). The diagram was produced based on data registered in the GWAS Catalog. The numbers in the figure indicate the numbers of genes in the different regions. The names of genes that are registered in association with at least two diseases and are highly expressed in lymphocytes but have unknown functions in the immune system are shown in the figure.

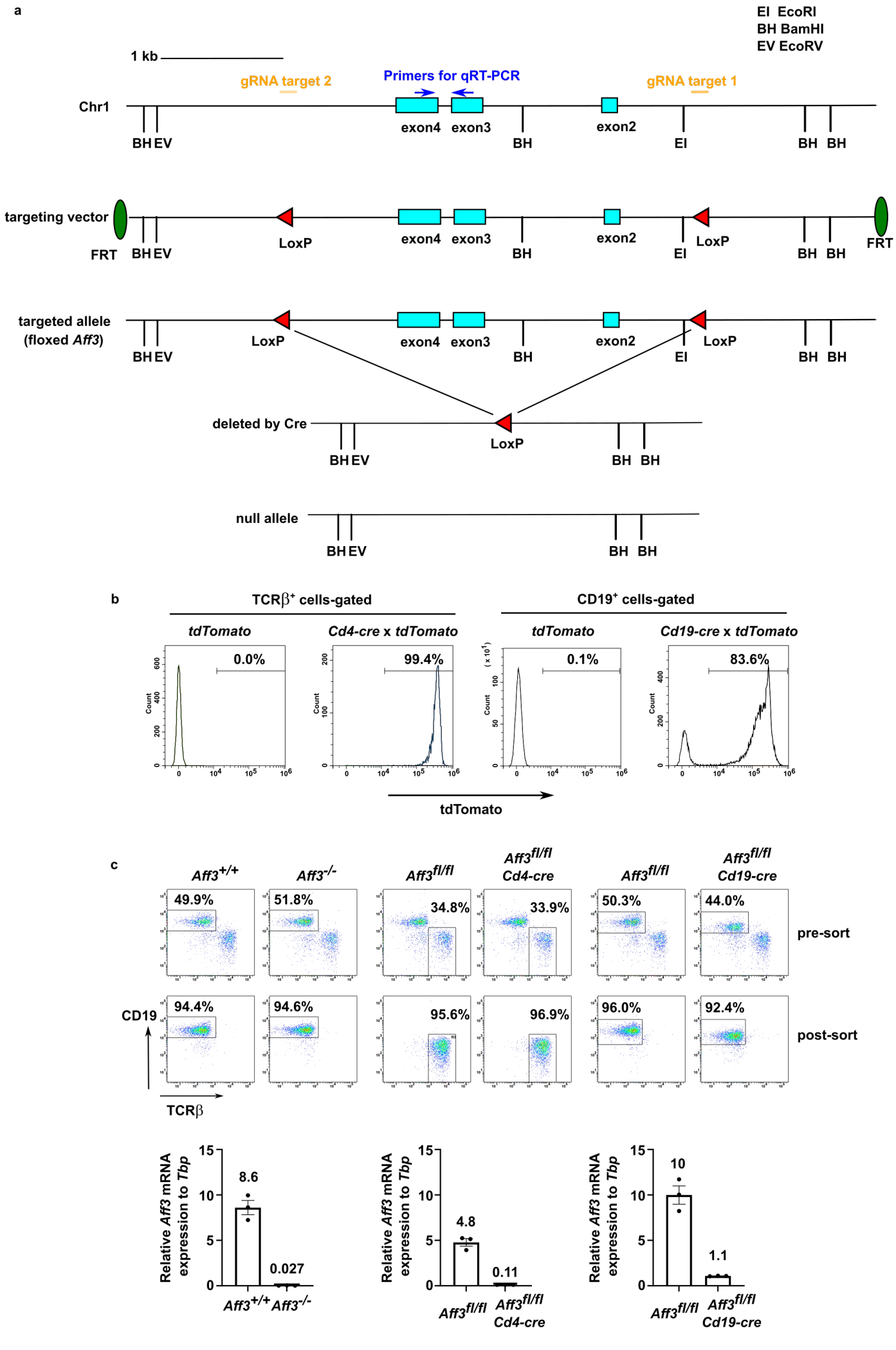
a
EI EcoRI
BH BamHI
EV EcoRV
1 kb
gRNA target 2
Primers for qRT-PCR
gRNA target 1
Chr1
BH EV
exon4 exon3
BH
exon2
EI
BH BH
targeting vector
FRT
LoxP
FRT
targeted allele
(floxed Aff3)
deleted by Cre
null allele
b
TCRβ+ cells-gated
CD19+ cells-gated
tdTomato
Cd4-cre x tdTomato
Cd19-cre x tdTomato
0.0%
99.4%
0.1%
83.6%
Count
tdTomato
c
Aff3+/+
Aff3-/-
Aff3fl/fl
Aff3fl/fl Cd4-cre
Aff3fl/fl Cd19-cre
49.9%
51.8%
34.8%
33.9%
50.3%
44.0%
pre-sort
CD19
94.4%
94.6%
95.6%
96.9%
96.0%
92.4%
post-sort
TCRβ
Relative Aff3 mRNA expression to Tbp
8.6
0.027
4.8
0.11
10
1.1

Fig. S2. (a) Schematic diagram of the mouse *Aff3* gene locus and the CRISPR–Cas9 strategy used to create the *Aff3*-null and floxed-*Aff3* alleles. The knock-in of the LoxP fragment and the deletion of exons were confirmed by PCR cloning and sequencing of this region. The deletion from exons 2 to 4 induces a frameshift and results in the production of a small protein consisting of 17 amino acids of the AFF3 N-terminus and 14 amino acids resulting from the frameshift. The positions of the gRNAs and the primers used for qRT–PCR in (c) are shown at the top. (b) The efficiency of Cre-mediated deletion was assessed by using Rosa26-*loxP*-flanked stop cassette-tdTomato ($R26^{LSL\text{-}tdTomato}$) mice as reporters. Spleen TCRβ$^+$ T cells (for *Cd4-cre*) or spleen CD19$^+$ cells (for *Cd19-cre*) were gated and examined for the expression of tdTomato. (c) Efficiency of *Aff3* gene deletion. B or T cells were purified from the spleens of mice of each genotype by magnet sorting. The purity of the cells was verified by flow cytometry (upper panels). Total RNA was extracted from the purified cells and used for qRT–PCR. *Aff3* mRNA expression was normalized to *Tbp* mRNA expression (lower panels). $Aff3^{fl/fl}$, $Aff3^{fl/fl}$ *Cd4-cre*$^+$, and *Aff3fl/fl Cd19-cre*$^+$ indicate floxed *Aff3*, floxed *Aff3* crossed with *Cd4-cre*, and floxed *Aff3* crossed with *Cd19-cre* mice, respectively. The primers used in the experiments are indicated in (a) and listed in Table S4.

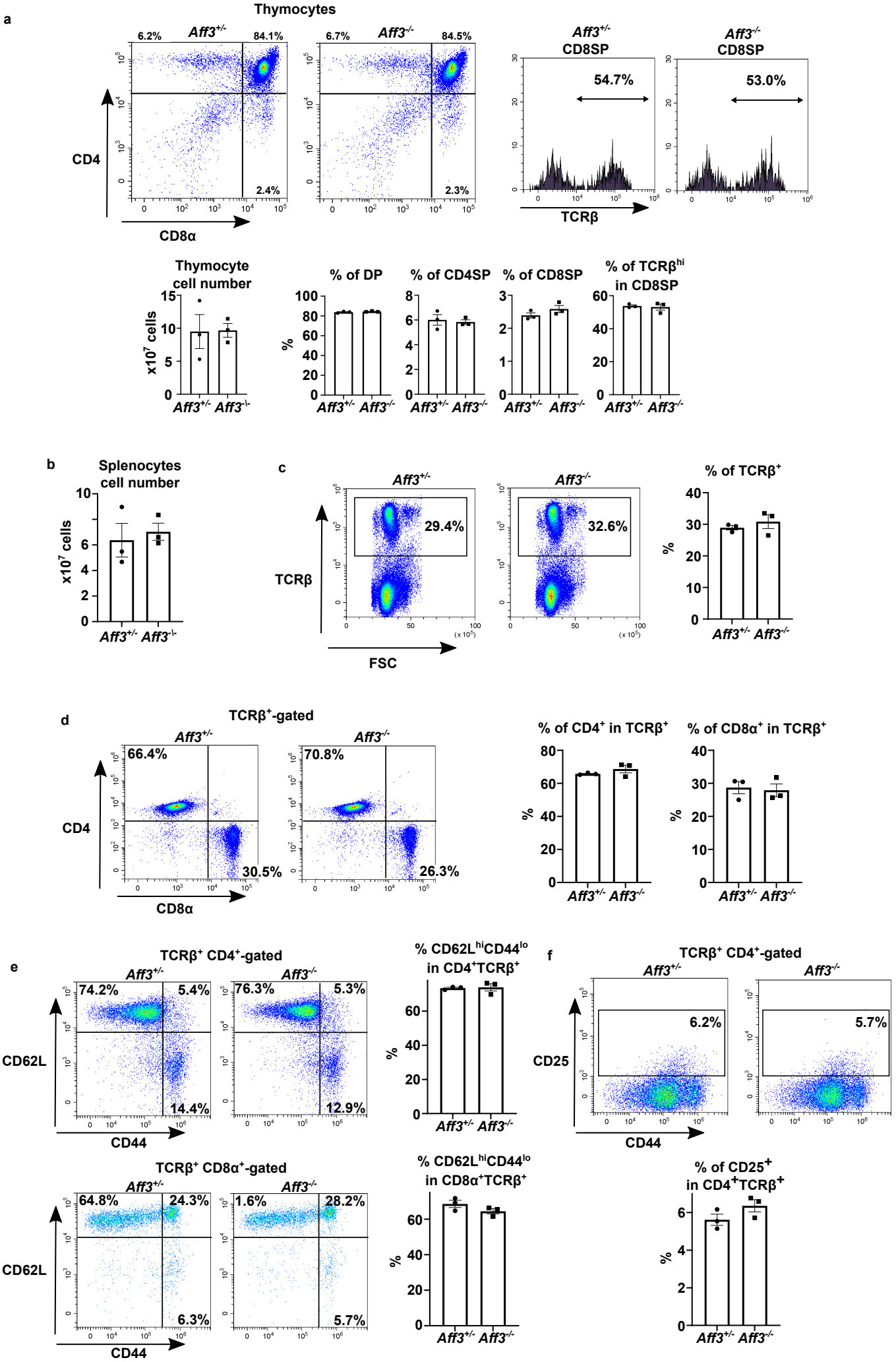
a
Thymocytes
Aff3+/-
Aff3-/-
6.2%
84.1%
2.4%
6.7%
84.5%
2.3%
CD4
CD8α
CD8SP
54.7%
53.0%
TCRβ
Thymocyte cell number
x10^7 cells
% of DP
% of CD4SP
% of CD8SP
% of TCRβhi in CD8SP
%
b
Splenocytes cell number
c
29.4%
32.6%
% of TCRβ+
FSC
d
TCRβ+-gated
66.4%
30.5%
70.8%
26.3%
% of CD4+ in TCRβ+
% of CD8α+ in TCRβ+
e
TCRβ+ CD4+-gated
74.2%
5.4%
14.4%
76.3%
5.3%
12.9%
CD62L
CD44
% CD62LhiCD44lo in CD4+TCRβ+
TCRβ+ CD8α+-gated
64.8%
24.3%
6.3%
1.6%
28.2%
5.7%
% CD62LhiCD44lo in CD8α+TCRβ+
f
6.2%
5.7%
CD25
% of CD25+ in CD4+TCRβ+

Fig. S3. Effects of *Aff3* deficiency on T-cell populations. (a) Analysis of thymocytes and T-cell subpopulations (n=3 in each group). (b-f) Analysis of splenocytes. (b) Number of splenocytes (n=3 in each group). (c) Flow cytometry analysis of T cells in the splenocyte population (n=3 in each group). (d) CD4 and CD8α profiles of $TCR\beta^+$-gated cells (n=3 in each group). (e) CD62L and CD44 profiles of $TCR\beta^+$- and $CD4^+$- or $CD8^+$-gated T cells (n=3 in each group). (f) CD25 expression in $TCRb^+CD4^+$ T cells (n=3 in each group). The data are shown as the mean ± SEM. The P values were calculated using an unpaired t test with Welch's correction, but no significant differences ($p \leq 0.05$) were observed. The data shown in this figure are representative of two experiments.

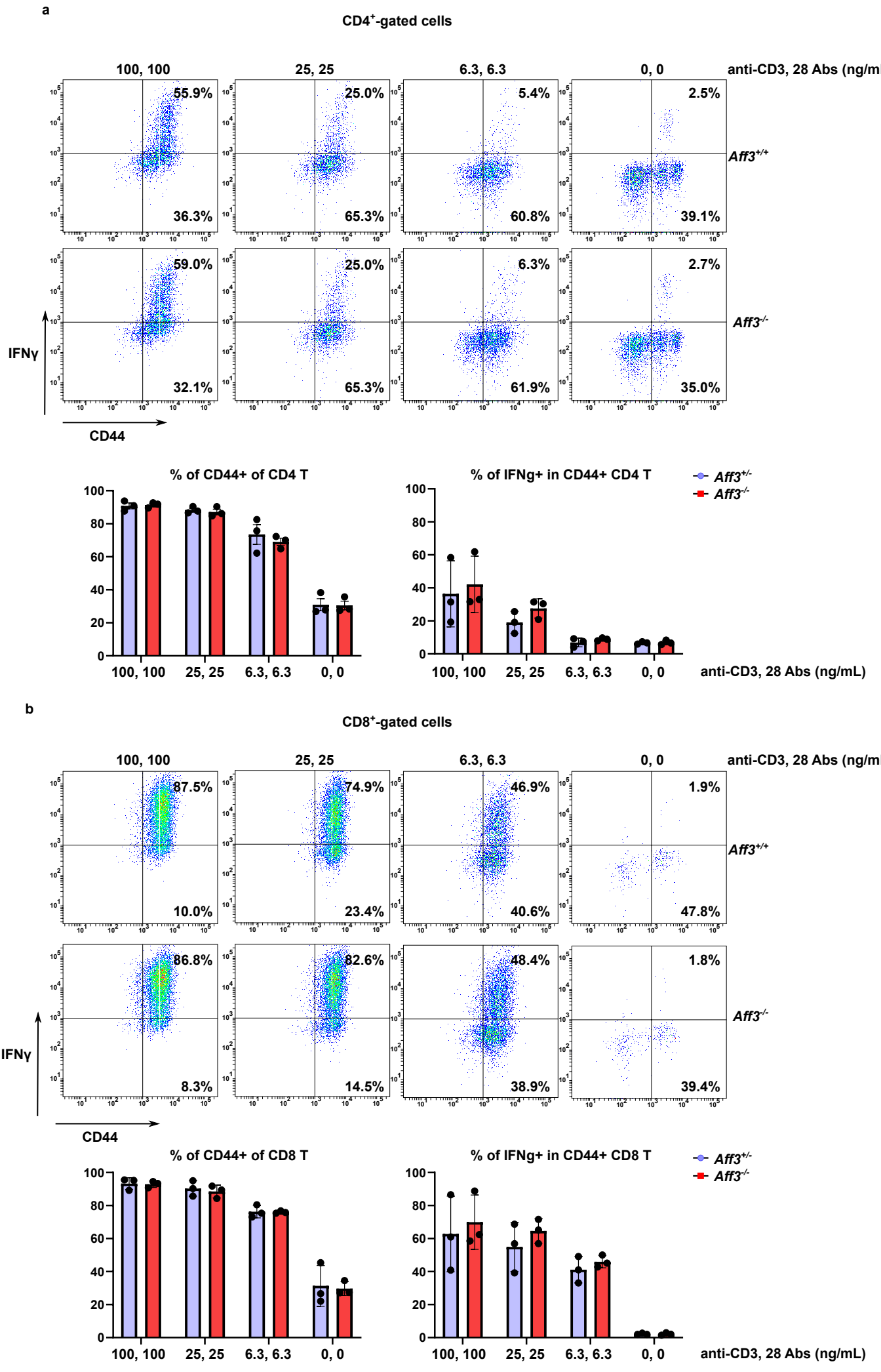
a
CD4+-gated cells
100, 100
25, 25
6.3, 6.3
0, 0
anti-CD3, 28 Abs (ng/mL)
55.9%
36.3%
25.0%
65.3%
5.4%
60.8%
2.5%
39.1%
Aff3+/+
59.0%
32.1%
25.0%
65.3%
6.3%
61.9%
2.7%
35.0%
Aff3-/-
IFNγ
CD44
% of CD44+ of CD4 T
% of IFNg+ in CD44+ CD4 T
Aff3+/-
Aff3-/-
b
CD8+-gated cells
87.5%
10.0%
74.9%
23.4%
46.9%
40.6%
1.9%
47.8%
86.8%
8.3%
82.6%
14.5%
48.4%
38.9%
1.8%
39.4%
% of CD44+ of CD8 T
% of IFNg+ in CD44+ CD8 T

Fig. S4. Effects of *Aff3* deficiency on (a) Th1 and (b) CTL cells. Splenocytes were cultured with anti-CD3 and soluble anti-CD28 antibodies at the indicated concentrations. After 3 days of culture, the cells were restimulated with PMA, ionomycin, and brefeldin A for 5 hours. Intracellular IFNγ expression was assessed by flow cytometry. The data shown in this figure are representative of three experiments. In all panels, the data are shown as the mean ± SEM.

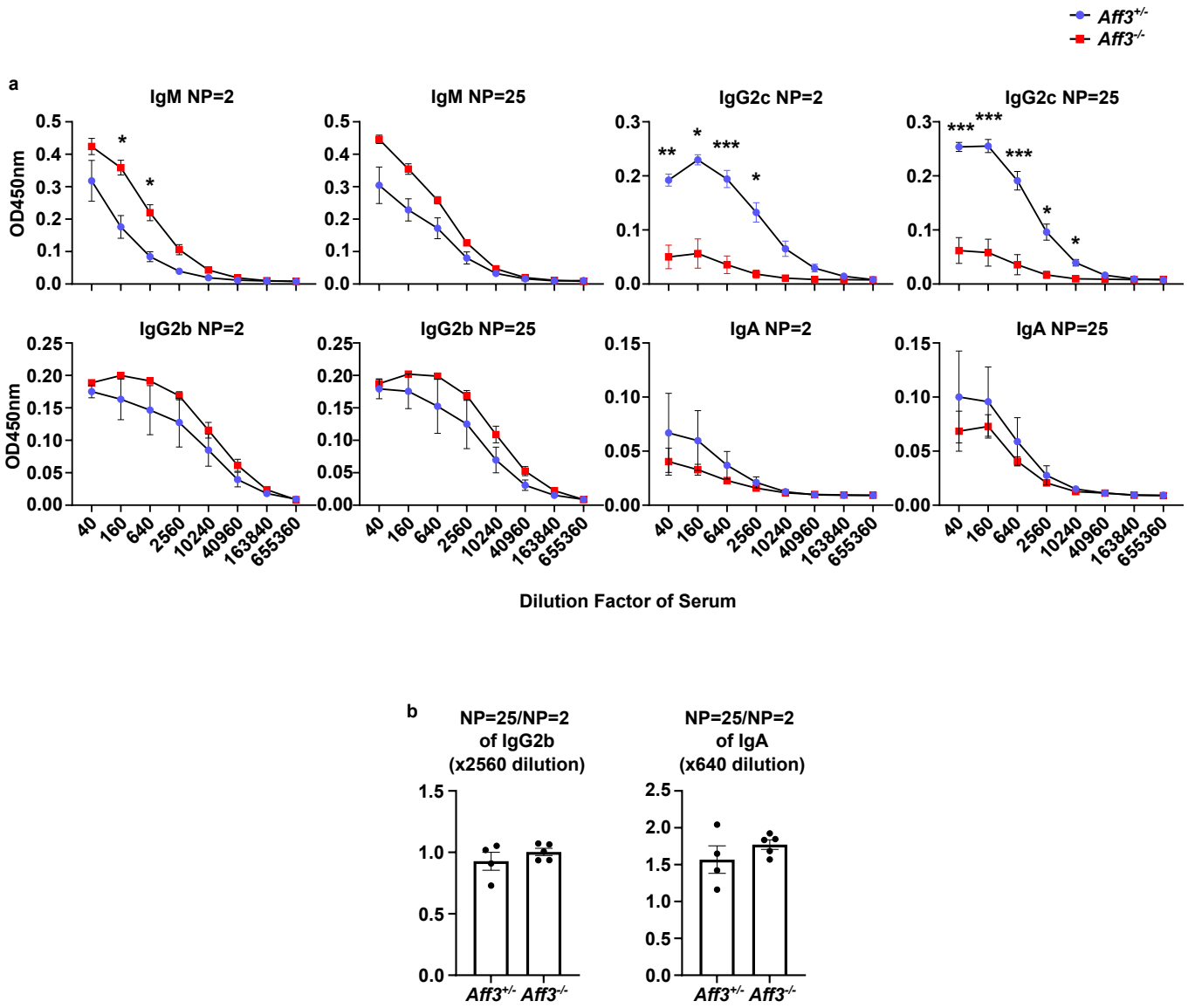
a
Aff3+/-
Aff3-/-
IgM NP=2
IgM NP=25
IgG2c NP=2
IgG2c NP=25
IgG2b NP=2
IgG2b NP=25
IgA NP=2
IgA NP=25
OD450nm
Dilution Factor of Serum
40
160
640
2560
10240
40960
163840
655360

b
NP=25/NP=2
of IgG2b
(x2560 dilution)
NP=25/NP=2
of IgA
(x640 dilution)
Aff3+/-
Aff3-/-

Fig. S5. Effects of *Aff3* deficiency on somatic hypermutation. Mice were immunized with NP-conjugated chicken gamma-globulin and complete Freund's adjuvant. Four weeks after immunization, the B-cell population and anti-NP antibodies were analyzed. (a) Anti-NP antibodies in serum ($Aff3^{+/-}$ n=4 [purple] and $Aff3^{-/-}$ n=5 [red]). NP=2 or NP=25 polymerized antigens were coated on the plate. The antibody titers were assessed by ELISA. (b) Statistical analysis of the ratios of anti-NP=25 to NP=2 antibody titers for IgG2b and IgA. The OD450 nm values of x2560 (IgG2b) or x640 (IgA) in Panel a were used for the analysis (n=4 or 5 in each group). In all panels, the data are shown as the mean ± SEM. *, **, ***, and **** indicate significant differences at $p<0.05$, 0.01, 0.005, and 0.001, respectively. The P values were calculated using multiple Welch's t tests with Holm–Sidak correction (a) or unpaired t tests with Welch's correction (b).

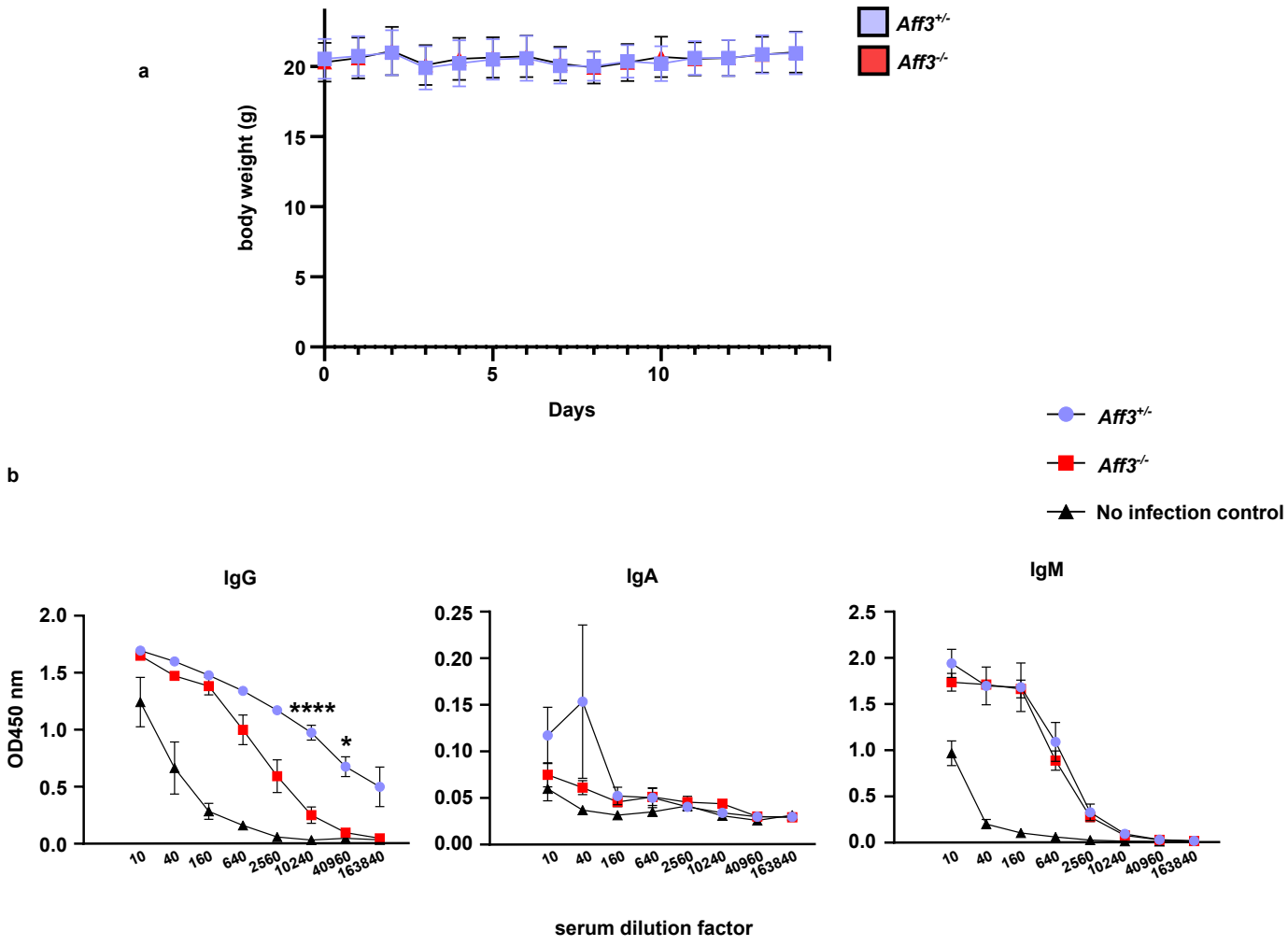
a
Aff3+/-
Aff3-/-
body weight (g)
0
5
10
15
20
0
5
10
Days
b
Aff3+/-
Aff3-/-
No infection control
IgG
IgA
IgM
OD450 nm
****
*
10
40
160
640
2560
10240
40960
163840
serum dilution factor

Fig. S6. Effects of *Aff3* deficiency on influenza infection in mice. (a) Body weights of mice after influenza virus infection (*Aff3*$^{+/-}$ (purple) and *Aff3*$^{-/-}$ (red), n=5 in each group). (b) Anti-influenza virus antibodies in serum were measured by ELISA at 14 days after infection (*Aff3*$^{+/-}$ n=5 [purple], *Aff3*$^{-/-}$ n=5 [red], and no-infection control n=2 [black]). In all panels, the data are shown as the mean ± SEM. *, **, ***, and **** indicate significant differences at $p<0.05$, 0.01, 0.005, and 0.001 between *Aff3*$^{+/-}$ and *Aff3*$^{-/-}$ mice, respectively. The P values were calculated using unpaired t tests with Welch's correction (a) or multiple Welch's t tests with Holm–Sidak correction (b).

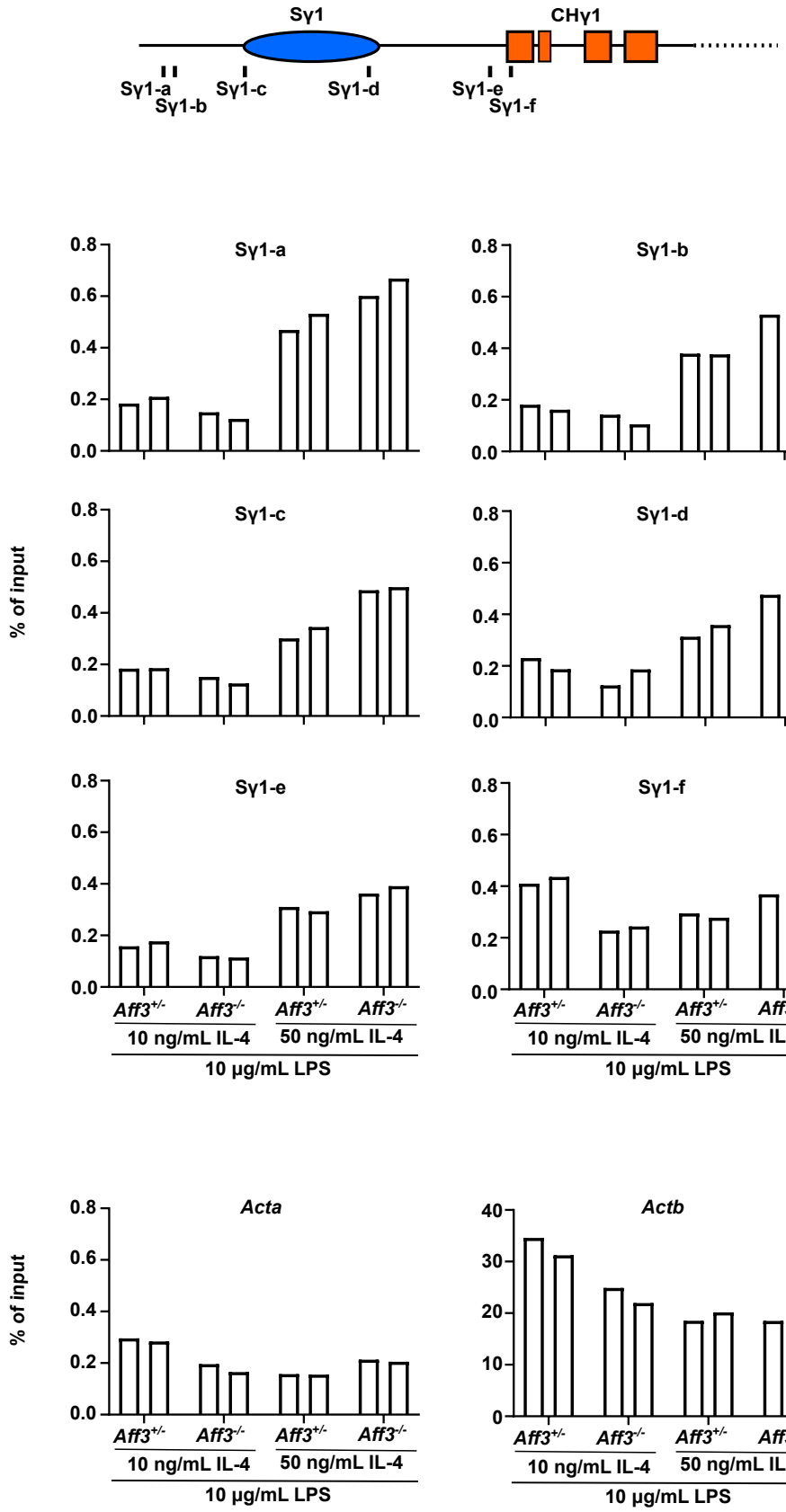
Sγ1
CHγ1
Sγ1-a
Sγ1-b
Sγ1-c
Sγ1-d
Sγ1-e
Sγ1-f
% of input
Sγ1-a
Sγ1-b
Sγ1-c
Sγ1-d
Sγ1-e
Sγ1-f
0.0
0.2
0.4
0.6
0.8
Aff3+/-
Aff3-/-
10 ng/mL IL-4
50 ng/mL IL-4
10 µg/mL LPS
Acta
Actb
0
10
20
30
40

Fig. S7. ChIP–qPCR analysis of RNA polymerase II. $CD43^-$ B cells were harvested from *Aff3*$^{+/-}$ or *Aff3*$^{-/-}$ mice and cultured in the presence of 10 μg/mL LPS and 10 ng/mL IL-4. After 2 days of culture, ChIP–qPCR was performed with an anti-RNA polymerase II antibody and the primers indicated in the diagram and Table S4. *Acta* and *Actb* were used as the negative and positive controls, respectively. Duplicate data for each sample are shown.

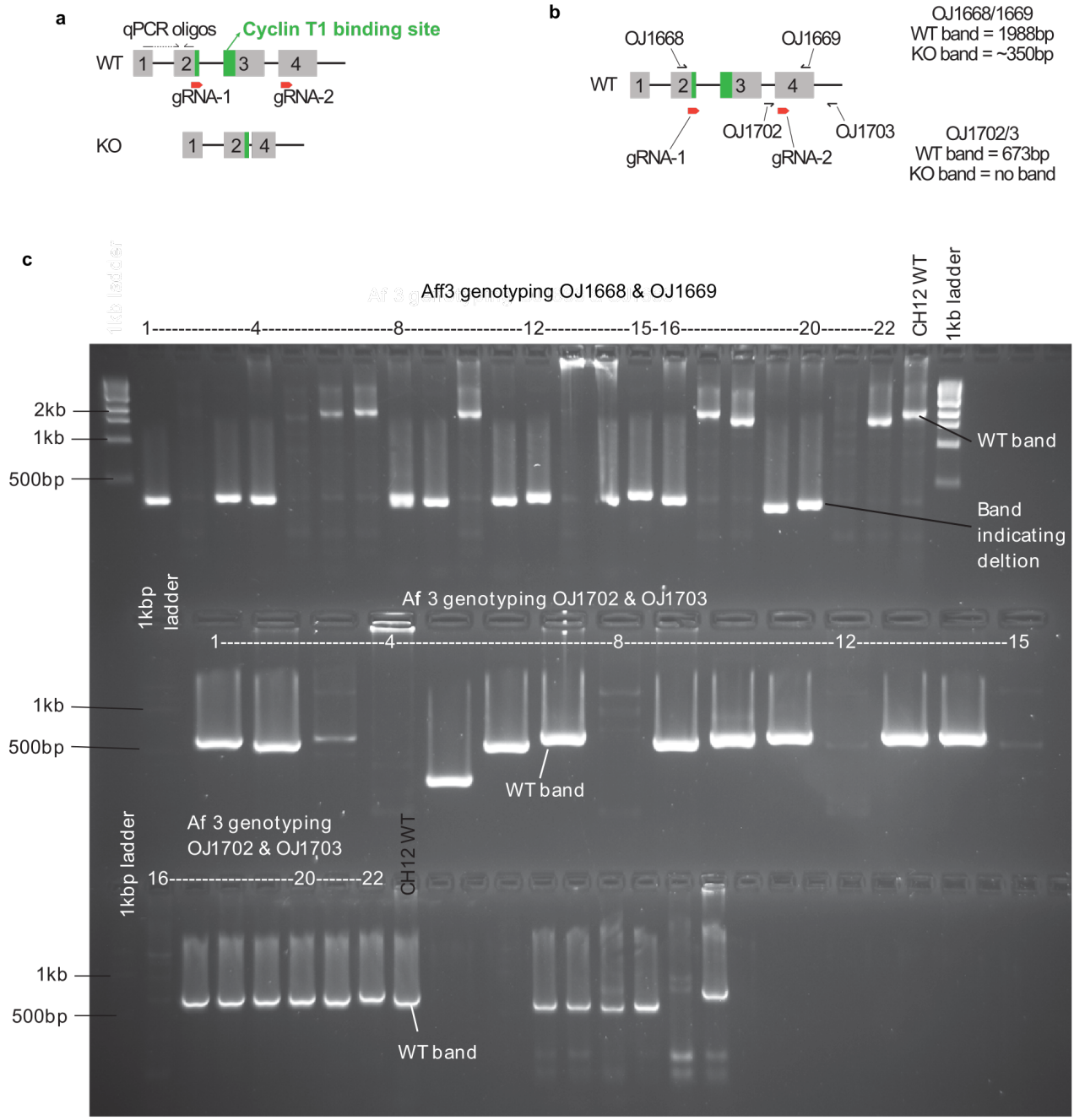
a
qPCR oligos
Cyclin T1 binding site
WT
1
2
3
4
gRNA-1
gRNA-2
KO
1
2
4
b
OJ1668
OJ1669
WT
1
2
3
4
OJ1702
OJ1703
gRNA-1
gRNA-2
OJ1668/1669
WT band = 1988bp
KO band = ~350bp
OJ1702/3
WT band = 673bp
KO band = no band
c
1kb ladder
Aff3 genotyping OJ1668 & OJ1669
1----------4----------8----------12----------15-16----------20--------22
CH12 WT
1kb ladder
2kb
1kb
500bp
WT band
Band indicating deltion
1kbp ladder
Af 3 genotyping OJ1702 & OJ1703
1----------4----------8----------12----------15
1kb
500bp
WT band
1kbp ladder
Af 3 genotyping
OJ1702 & OJ1703
16----------20-------22
CH12 WT
1kb
500bp
WT band

Fig. S8. Strategy of *Aff3* KO in CH12 cells. (a) Position of gRNA-1/2 and the predicted KO allele. The cyclin T1 binding site, which is thought to be important for AFF3 function, is shown in green. (b) Primers used for genotyping the *Aff3*-KO allele. The numbers in the gray boxes signify the exon numbers (a, b). (c) Agarose gel electrophoresis for genotyping. Clones 4, 15 and 16 were chosen for further analysis, as shown in Fig. 6. They were renamed clones 1, 2 and 3, respectively. The primers used in the experiments are listed in Table S4.

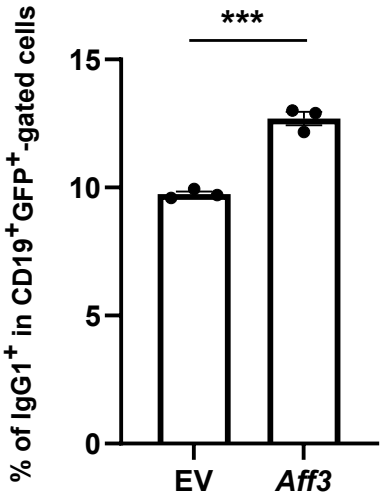
***
15
10
5
0
% of IgG1+ in CD19+GFP+-gated cells
EV
Aff3

Fig. S9. Overexpression of the AFF3 protein increases class switching to IgG1. $CD43^-$ B cells were harvested from *Aff3*$^{+/-}$ mice and cultured with LPS and IL-4. The cDNA of *Aff3* was transduced into the cells with a retroviral vector carrying the GFP marker. After 4 days of culture, the cells were analyzed by flow cytometry. GFP^+CD19^+ cells were gated, and the percentage of $IgG1^+$ cells was measured (n=3 in each group). EV indicates the empty vector. *Aff3* indicates the *Aff3* cDNA-containing vector. The data are shown as the mean ± SEM. *, **, ***, and **** indicate significant differences at $p<0.05$, 0.01, 0.005, and 0.001, respectively. The P values were calculated using unpaired t tests with Welch's correction. The data shown in this figure are representative of two experiments.

Extended Data Table 1. The rates of the swich regions in *Aff3* $^{+/-}$ and *Aff3* $^{-/-}$ B cells)

Mutations in IgM switch region

Aff3 $^{+/-}$

	mutated nucleotides	sequenced nucleotides	sequceded clone number
#1	8	5656	15
#2	3	2665	11
#3	3	4364	12
sum	**14**	**12685**	**38**
total mutation rate	0.0011037		

Aff3 $^{-/-}$

	mutated nucleotides	sequenced nucleotides	sequceded clone number
#1	9	4995	13
#2	6	3205	11
#3	5	4443	14
sum	**20**	**12643**	**38**
total mutation rate	0.0015819		

Mutations in IgG1 switch region

Aff3 $^{+/-}$

	mutated nucleotides	sequenced nucleotides	sequceded clone number
#1	6	4536	11
#2	5	3822	9
#3	3	2399	9
sum	**14**	**10757**	**29**
total mutation rate	0.0013015		

Aff3 $^{-/-}$

	mutated nucleotides	sequenced nucleotides	sequceded clone number
#1	2	9237	15
#2	0	2696	4
#3	0	4055	10
sum	**2**	**15988**	**29**
total mutation rate	0.0001251		

Extended Data Table 2. antibodies used in flow cytometry

Antibody	SOURCE	IDNETIFIER
PB anti-CD4 , clone RM4.5	Biolegend	100531
FITC anti-CD4, clone GK1.5	BD Biosciences	553729
V500 anti-CD8α, clone 53-6.7	Biolegend	100752
PE anti-TCRβ, clone H57-597	Biolegend	109208
PB anti-CD62L, clone MEL-14	Biolegend	104424
PECy7 anti-CD44, clone IM7	Biolegend	103030
APC anti-CD25, clone PC61.5	Invitrogen	47-0251-82
APC anti-IFNγ, clone XMG1.2	Biolegend	505810
PECy7 anti-CD19, clone 6D5	Biolegend	11520
APC anti-CD19, clone 6D5	Biolegend	115512
PECy7 anti-CD23, clone B3B4	Biolegend	101614
PE anti-CD21, clone eBio879	eBioscience	12-0211-083
PE anti-CD138, clone 281-2	BD Biosciences	553714
PB anti-CD73, clone TY/11.8	Biolegend	127217
APC anti-IgG1, clone RMG1-1	Biolegend	406609
BV421 anti-IgG3, clone R40-82	BD Biosciences	565808
biotin anti-IgG2c, clone 5.7	BD Biosciences	553504
APC streptavidin	Biolegend	405207
APC anti-CD86, clone PO3	Biolegend	105114

Extended Data Table 3. Catalog numbers of antibodies for ELISA

All antibodies in this table were purchaced from Bethyl laboratories

	capture antibody	dection antibody (HRP-cojugated)
IgM	goat polyclonal (Cat. No. A90-101A)	goat polyclonal (Cat. No. A90-101P)
IgG1	goat polyclonal (Cat. No. A90-105A)	goat polyclonal (Cat. No. A90-105P)
IgG2b	goat polyclonal (Cat. No. A90-109A)	goat polyclonal (Cat. No. A90-109P)
IgG2c	goat polyclonal (Cat. No. A90-136A)	goat polyclonal (Cat. No. A90-136P)
IgG3	goat polyclonal (Cat. No. A90-111A)	goat polyclonal (Cat. No. A90-111P)
IgA	goat polyclonal (Cat. No. A90-103A)	goat polyclonal (Cat. No. A90-103P)

Extended Data Table 4. oligonucleotides used in this paper

Oligonucleotide	Sequence	Reference
Aff3 fwd for cloning (Fig3d)	CCCACCATGGACAGCTTC	
Aff3 rev for cloning (Fig3d)	CAGTCTGGCTCAAAGGCTTG	
Aff1 fwd for cloning (Fig3d)	CACTTAATGGAAACGAGGATTCTC	
Aff1 rev for cloning (Fig3d)	CTTCCAATGGTGCAGAGACA	
Aff4 fwd for cloning (Fig3d)	AACATGAACCGTGAAGACCGG	
Aff4 rev for cloning (Fig3d)	TGGCAGTTTTCCTTTGTGATG	
Aicda fwd (Fig4c)	ATCGGGATCATGACCTTCAA	
Aicda rev (Fig4c)	GCCGAAGTTGTCTGGTTAGC	
Acta fwd (Fig4d, FigS7)	CTTCTCCATGTCGTCCCAGT	
Acta rev (Fig4d, FigS7)	GGACTCCTACGTGGGTGATG	
Sμ SR fwd (Fig4d)	TGGCCAGAACCAGAATCAATT	Xu J *et al.* (70)
Sμ SR rev (Fig4d)	GCCTCACATAATCCATGTCAGCTA	Xu J *et al.* (70)
Tbp fwd (Fig4c, 5a, S2c)	CTCAGTTACAGGTGGCAGCA	
Tbp rev (Fig4c, 5a, S2c)	CAGCACAGAGCAAGCAACTC	
Sγ1-c fwd (Fig4d, FigS7)	CCTCAGCTCTTTTGCAGGTG	
Sγ1-c rev (Fig4d, FigS7)	AAGTAGAGGGAAGCCCAAGC	
Sγ1-d fwd (Fig4d, FigS7)	CTTGCTCCTAAGGCACTGCT	
Sγ1-d rev (Fig4d, FigS7)	CAGCCAGGAGAAATGGAAGA	
Sγ1 germline fwd (Fig5a)	GGATCCAGAGTTCCAGGTCACT	
Sγ1 germline rev (Fig5a)	GGCCTCCTAGACAAGCACAG	
Sγ1 postswitch fwd (Fig5a)	TCTGGACCTCTCCGAAACCA	Lin L *et al.* (71)
Sγ1 postswitch rev (Fig5a)	GGATCCAGAGTTCCAGGTCACT	Wang NS *et al*. (72)
Sμ-Sγ1-SR fwd (Fig5b)	AATGGATACCTCAGTGGTTTTTAATGGTGGGTTTA	Reina-San-Martin B *et al.* (73)
Sμ-Sγ1-SR rev (Fig5b)	AACTACTAAACTTGTACCTGTCCTGGCACC	Denkelmann M *et al.* (74)
Cd19 fwd (Fig5b)	AATGTTGTGCTGCCATGCCTC	Rickert RC *et al.* (75)
Cd19 rev (Fig5b)	GTCTGAAGCATTCCACCGGAA	Rickert RC *et al.* (75)
Aicda for qRT-PCR (Fig6a)	GCCACCTTCGCAACAAGTCT	
Aicda for qRT-PCR (Fig6a)	CCGGGCACAGTCATAGCAC	
Sμ GLT fwd for qRT-PCR (Fig6a)	TAGTAAGCGAGGCTCTAAAAAGCAC	
Sμ GLT rev for qRT-PCR (Fig6a)	ACTCAGAGAAGCCCACCCAT	
Sα GLT fwd for qRT-PCR(Fig6a)	GGCTAGAATGGGCTAGAGTGAGTTA	
Sα GLT rev for qRT-PCR(Fig6a)	GCCTATTTTGGCCAGTCTACTTAC	
Sμ-P fwd (Fig6d)	CCACCTGGGTAATTTGCATTTC	Methot *et al* (52)
Sμ-P rev (Fig6d)	GGGAAACTAGAACTACTCAAGCTAA	Methot et al (52)
Sμ-a fwd (Fig6d)	TAGTAAGCGAGGCTCTAAAAAGCAC	Cortizas *et al* (76)
Sμ-a rev (Fig6d)	ACTCAGAGAAGCCCACCCAT	Cortizas et al (76)
Sμ-b fwd (Fig6d)	GGTTGGGAGACCATGAATTG	Cortizas et al (76)
Sμ-b rev (Fig6d)	TTCTTAGCTCAACCCAGTTTATCC	Cortizas et al (76)
Sα-a fwd (Fig6d)	AAGCAGGCCTGGGGTGGACA	Methot et al (52)
Sα-a rev (Fig6d)	AGCAAGCTCAGCCCAGCCTAA	Methot et al (52)
Sα-b fwd (Fig6d)	CTTGGCTAGGCTACAATGGATTGAGC	Cortizas et al (76)
Sα-b rev (Fig6d)	GTGCAACTCTATCTAGGTCTGCCCGGT	Cortizas et al (76)
gRNA *Aff3* target 1 (FigS2a)	CCTCGTGAGGGGGATGACATTCC	
gRNA *Aff3* target 2 (FigS2a)	CCACTCGATAGGTCGCAGGAAAG	
Aff3 fwd for qRT-PCR (FigS2a,S2c)	CACCGTCCGATGGCCAACA	
Aff3 rev for qRT-PCR (FigS2a, S2c)	GGGGGAAAGTTCTGAACACA	
Sγ1-a fwd (FigS7)	CCTGTAGTCCATGCCAAACA	
Sγ1-a rev (FigS7)	GGCCTCCTAGACAAGCACAG	
Sγ1-b fwd (FigS7)	TGCAGGTCTTGTGTCCTGAG	
Sγ1-b rev (FigS7)	TCCCAGCATTGGGATTAGAG	
Sγ1-e fwd (FigS7)	TCTGATGTGGGCATCTGTGT	
Sγ1-e rev (FigS7)	GATGTGCCGACTTCAATGTG	
Sγ1-f fwd (FigS7)	GGATCCAGAGTTCCAGGTCA	
Sγ1-f rev (FigS7)	CGACACCCCCATCTGTCTAT	
Actb fwd (FigS7)	CAGCTTCTTTGCAGCTCCTT	
Actb rev (FigS7)	GGACCCTGCAGTGAGGTACT	
gRNA *Aff3* exon 2 target sequence (FigS8)	AGCGAACCCTACAAGGTAGA	
gRNA *Aff3* exon 4 target sequence (FigS8)	AAGTGTGCAATATGGAGACG	
genotyping *Aff3* OJ1668 (FigS8)	TCAGATGTACATGACTTTGGGC	
genotyping *Aff3* OJ1669 (FigS8)	TTAGGAGATTCGTCAGGAGCTT	
genotyping *Aff3* OJ1703 (FigS8)	GCCACAATGCAAAACCTGTTCA	
genotyping *Aff3* OJ1703 (FigS8)	AGGAGGCATTCCATCGCTAAGT	

Extended Data Table 5. abbrevation of cell types in Fig7a

naive CD4	naive CD4 cells
Mem CD4	Memory CD4 cells
Th1	T helper 1 cells
Th2	T helper 2 cells
Th17	T hlper 17 cells
Tfh	T follicular helper cells
Fr. I nTreg	Fraction I naive regulatory T cells
Fr. II eTreg	Fraction II effector regulatory T cellls
Fr. III T	Fraction III non-regulatory T cells
Naive CD8	Naive CD8
CM CD8	Central memory CD8 T cells
EM CD8	Effctor memory CD8 T cells
TEMRA CD8	CD8+ effector memory CD45RA+ cells
NK	Natural killer cells
Naive B	Naive B cells
USM B	Unswitched memory B cells
SM B	Switched meory B cells
Plasmablast	Plasmablasts
DN B	Dobule nagative B cells (IgD-negative, CD27-negative)
CL Mono	Clasical monocytes
CD16p Mono	CD16 positive monocytes
Int Mono	Intermediated monocytes
NC Mono	Non-classical monocytes
mDC	Myeloid dendritic cells
pDC	Plasmacytoid dendritic cells
Neu	Neutrophils
LDG	Low-density granulocytes

REFERENCES AND NOTES

1. W. R. Reay, M. J. Cairns, Advancing the use of genome-wide association studies for drug repurposing. *Nat. Rev. Genet.* **22**, 658–671 (2021).

2. M. Claussnitzer, J. H. Cho, R. Collins, N. J. Cox, E. T. Dermitzakis, M. E. Hurles, S. Kathiresan, E. E. Kenny, C. M. Lindgren, D. G. MacArthur, K. N. North, S. E. Plon, H. L. Rehm, N. Risch, C. N. Rotimi, J. Shendure, N. Soranzo, M. I. McCarthy, A brief history of human disease genetics. *Nature* **577**, 179–189 (2020).

3. X. Bai, J. Kim, Z. Yang, M. J. Jurynec, T. E. Akie, J. Lee, J. LeBlanc, A. Sessa, H. Jiang, A. DiBiase, Y. Zhou, D. J. Grunwald, S. Lin, A. B. Cantor, S. H. Orkin, L. I. Zon, TIF1γ controls erythroid cell fate by regulating transcription elongation. *Cell* **142**, 133–143 (2010).

4. V. Cavalleri, L. R. Bettini, C. Barboni, A. Cereda, M. Mariani, M. Spinelli, C. Gervasini, S. Russo, A. Biondi, M. Jankovic, A. Selicorni, Thrombocytopenia and Cornelia de Lange syndrome: Still an enigma? *Am. J. Med. Genet. A.* **170**, 130–134 (2016).

5. A. Al Ismail, A. Husain, M. Kobayashi, T. Honjo, N. A. Begum, Depletion of recombination-specific cofactors by the C-terminal mutant of the activation-induced cytidine deaminase causes the dominant negative effect on class switch recombination. *Int. Immunol.* **29**, 525–537 (2017).

6. R. Casellas, U. Basu, W. T. Yewdell, J. Chaudhuri, D. F. Robbiani, J. M. Di Noia, Mutations, kataegis and translocations in B cells: Understanding AID promiscuous activity. *Nat. Rev. Immunol.* **16**, 164–176 (2016).

7. P. B. Chen, H. V. Chen, D. Acharya, O. J. Rando, T. G. Fazzio, R loops regulate promoter-proximal chromatin architecture and cellular differentiation. *Nat. Struct. Mol. Biol.* **22**, 999–1007 (2015).

8. K. Assing, C. Nielsen, M. Kirchhoff, H. O. Madsen, L. P. Ryder, N. Fisker, CD4+ CD31+ recent thymic emigrants in CHD7 haploinsufficiency (CHARGE syndrome): A case. *Hum. Immunol.* **74**, 1047–1050 (2013).

9. S. Bottardi, L. Mavoungou, E. Milot, IKAROS: A multifunctional regulator of the polymerase II transcription cycle. *Trends Genet.* **31**, 500–508 (2015).

10. W. J. Astle, H. Elding, T. Jiang, D. Allen, D. Ruklisa, A. L. Mann, D. Mead, H. Bouman, F. Riveros-Mckay, M. A. Kostadima, J. J. Lambourne, S. Sivapalaratnam, K. Downes, K. Kundu, L. Bomba, K. Berentsen, J. R. Bradley, L. C. Daugherty, O. Delaneau, K. Freson, S. F. Garner, L. Grassi, J. Guerrero, M. Haimel, E. M. Janssen-Megens, A. Kaan, M. Kamat, B. Kim, A. Mandoli, J. Marchini, J. H. A. Martens, S. Meacham, K. Megy, J. O'Connell, R. Petersen, N. Sharifi, S. M. Sheard, J. R. Staley, S. Tuna, M. van der Ent, K. Walter, S.-Y. Wang, E. Wheeler, S. P. Wilder, V. Iotchkova, C. Moore, J. Sambrook, H. G. Stunnenberg, E. Di Angelantonio, S. Kaptoge, T. W. Kuijpers, E. Carrillo-de-Santa-Pau, D. Juan, D. Rico, A. Valencia, L. Chen, B. Ge, L. Vasquez, T. Kwan, D. Garrido-Martín, S. Watt, Y. Yang, R. Guigo, S. Beck, D. S. Paul, T. Pastinen, D. Bujold, G. Bourque, M. Frontini, J. Danesh, D. J. Roberts, W. H. Ouwehand, A. S. Butterworth, N. Soranzo, The allelic landscape of human blood cell trait variation and links to common complex disease. *Cell* **167**, 1415–1429.e19 (2016).

11. C. Polychronakos, Q. Li, Understanding type 1 diabetes through genetics: Advances and prospects. *Nat. Rev. Genet.* **12**, 781–792 (2011).

12. C. Ma, L. M. Staudt, LAF-4 encodes a lymphoid nuclear protein with transactivation potential that is homologous to AF-4, the gene fused to MLL in t(4;11) leukemias. *Blood* **87**, 734–745 (1996).

13. M. Hiwatari, T. Taki, T. Taketani, M. Taniwaki, K. Sugita, M. Okuya, M. Eguchi, K. Ida, Y. Hayashi, Fusion of an AF4-related gene, LAF4, to MLL in childhood acute lymphoblastic leukemia with t(2;11)(q11;q23). *Oncogene* **22**, 2851–2855 (2003).

14. Z. Luo, C. Lin, E. Guest, A. S. Garrett, N. Mohaghegh, S. Swanson, S. Marshall, L. Florens, M. P. Washburn, A. Shilatifard, The super elongation complex family of RNA polymerase II elongation factors: Gene target specificity and transcriptional output. *Mol. Cell. Biol.* **32**, 2608–2617 (2012).

15. N. He, M. Liu, J. Hsu, Y. Xue, S. Chou, A. Burlingame, N. J. Krogan, T. Alber, Q. Zhou, HIV-1 Tat and host AFF4 recruit two transcription elongation factors into a bifunctional complex for coordinated activation of HIV-1 transcription. *Mol. Cell* **38**, 428–438 (2010).

16. F. X. Chen, E. R. Smith, A. Shilatifard, Born to run: Control of transcription elongation by RNA polymerase II. *Nat. Rev. Mol. Cell Biol.* **19**, 464–478 (2018).

17. ENCODE Project Consortium, An integrated encyclopedia of DNA elements in the human genome. *Nature* **489**, 57–74 (2012).

18. Z. Luo, C. Lin, A. R. Woodfin, E. T. Bartom, X. Gao, E. R. Smith, A. Shilatifard, Regulation of the imprinted Dlk1-Dio3 locus by allele-specific enhancer activity. *Genes Dev.* **30**, 92–101 (2016).

19. Y. Zhang, C. Wang, X. Liu, Q. Yang, H. Ji, M. Yang, M. Xu, Y. Zhou, W. Xie, Z. Luo, C. Lin, AFF3-DNA methylation interplay in maintaining the mono-allelic expression pattern of *XIST* in terminally differentiated cells. *J. Mol. Cell Biol.*, 761–769 (2019).

20. D. S. W. Lee, O. L. Rojas, J. L. Gommerman, B cell depletion therapies in autoimmune disease: Advances and mechanistic insights. *Nat. Rev. Drug Discov.* **20**, 179–199 (2021).

21. S. J. S. Rubin, M. S. Bloom, W. H. Robinson, B cell checkpoints in autoimmune rheumatic diseases. *Nat. Rev. Rheumatol.* **15**, 303–315 (2019).

22. T. Saha, D. Sundaravinayagam, M. Di Virgilio, Charting a DNA repair roadmap for immunoglobulin class switch recombination. *Trends Biochem. Sci.* **46**, 184–199 (2021).

23. Z. Chen, J. H. Wang, Signaling control of antibody isotype switching. *Adv. Immunol.* **141**, 105–164 (2019).

24. Y. Feng, N. Seija, J. M. Di Noia, A. Martin, AID in antibody diversification: There and back again. *Trends Immunol.* **41**, 586–600 (2020).

25. K. Yu, M. R. Lieber, Current insights into the mechanism of mammalian immunoglobulin class switch recombination. *Crit. Rev. Biochem. Mol. Biol.* **54**, 333–351 (2019).

26. A. L. Kenter, S. Kumar, R. Wuerffel, F. Grigera, AID hits the jackpot when missing the target. *Curr. Opin. Immunol.* **39**, 96–102 (2016).

27. M. D. Fortune, H. Guo, O. Burren, E. Schofield, N. M. Walker, M. Ban, S. J. Sawcer, J. Bowes, J. Worthington, A. Barton, S. Eyre, J. A. Todd, C. Wallace, Statistical colocalization of genetic risk variants for related autoimmune diseases in the context of common controls. *Nat. Genet.* **47**, 839–846 (2015).

28. S. N. Lewis, E. Nsoesie, C. Weeks, D. Qiao, L. Zhang, Prediction of disease and phenotype associations from genome-wide association studies. *PLOS ONE* **6**, e27175 (2011).

29. A. Hertweck, C. M. Evans, M. Eskandarpour, J. C. H. Lau, K. Oleinika, I. Jackson, A. Kelly, J. Ambrose, P. Adamson, D. J. Cousins, P. Lavender, V. L. Calder, G. M. Lord, R. G. Jenner, T-bet activates Th1 genes through mediator and the super elongation complex. *Cell Rep.* **15**, 2756–2770 (2016).

30. R. Chen, S. Bélanger, M. A. Frederick, B. Li, R. J. Johnston, N. Xiao, Y.-C. Liu, S. Sharma, B. Peters, A. Rao, S. Crotty, M. E. Pipkin, In vivo RNA interference screens identify regulators of antiviral CD4(+) and CD8(+) T cell differentiation. *Immunity* **41**, 325–338 (2014).

31. C. Demarta-Gatsi, L. Smith, S. Thiberge, R. Peronet, P. H. Commere, M. Matondo, L. Apetoh, P. Bruhns, R. Ménard, S. Mécheri, Protection against malaria in mice is induced by blood stage-arresting histamine-releasing factor (HRF)-deficient parasites. *J. Exp. Med.* **213**, 1419–1428 (2016).

32. W. I. White, C. B. Evans, D. W. Taylor, Antimalarial antibodies of the immunoglobulin G2a isotype modulate parasitemias in mice infected with Plasmodium yoelii. *Infect. Immun.* **59**, 3547–3554 (1991).

33. S. Waki, S. Uehara, K. Kanbe, H. Nariuch, M. Suzuki, Interferon-gamma and the induction of protective IgG2a antibodies in non-lethal Plasmodium berghei infections of mice. *Parasite Immunol.* **17**, 503–508 (1995).

34. R. A. Cavinato, K. R. B. Bastos, L. R. Sardinha, R. M. Elias, J. M. Alvarez, M. R. D'Império Lima, Susceptibility of the different developmental stages of the asexual (schizogonic) erythrocyte cycle of *Plasmodium chabaudi chabaudi* to hyperimmune serum, immunoglobulin (Ig)G1, IgG2a and $F(ab')_2$ fragments. *Parasite Immunol.* **23**, 587–597 (2001).

35. Q. Wang, K. R. Kieffer-Kwon, T. Y. Oliveira, C. T. Mayer, K. Yao, J. Pai, Z. Cao, M. Dose, R. Casellas, M. Jankovic, M. C. Nussenzweig, D. F. Robbiani, The cell cycle restricts activation-induced cytidine deaminase activity to early G1. *J. Exp. Med.* **214**, 49–58 (2017).

36. S. Chou, H. Upton, K. Bao, U. Schulze-Gahmen, A. J. Samelson, N. He, A. Nowak, H. Lu, N. J. Krogan, Q. Zhou, T. Alber, HIV-1 Tat recruits transcription elongation factors dispersed along a flexible AFF4 scaffold. *Proc. Natl. Acad. Sci. U.S.A.* **110**, E123–E131 (2013).

37. S. Qi, Z. Li, U. Schulze-Gahmen, G. Stjepanovic, Q. Zhou, J. H. Hurley, Structural basis for ELL2 and AFF4 activation of HIV-1 proviral transcription. *Nat. Commun.* **8**, 14076 (2017).

38. N. He, C. K. Chan, B. Sobhian, S. Chou, Y. Xue, M. Liu, T. Alber, M. Benkirane, Q. Zhou, Human polymerase-associated factor complex (PAFc) connects the super elongation complex (SEC) to RNA polymerase II on chromatin. *Proc. Natl. Acad. Sci. U.S.A.* **108**, E636–E645 (2011).

39. R. Pavri, R loops in the regulation of antibody gene diversification. *Genes* **8**, 154 (2017).

40. C. Ribeiro de Almeida, S. Dhir, A. Dhir, A. E. Moghaddam, Q. Sattentau, A. Meinhart, N. J. Proudfoot, RNA helicase DDX1 converts RNA G-quadruplex structures into R-loops to promote IgH class switch recombination. *Mol. Cell* **70**, 650–662.e8 (2018).

41. N. A. Begum, N. Izumi, M. Nishikori, H. Nagaoka, R. Shinkura, T. Honjo, Requirement of non-canonical activity of uracil DNA glycosylase for class switch recombination. *J. Biol. Chem.* **282**, 731–742 (2007).

42. W. T. Yewdell, Y. Kim, P. Chowdhury, C. M. Lau, R. M. Smolkin, K. T. Belcheva, K. C. Fernandez, M. Cols, W. F. Yen, B. Vaidyanathan, D. Angeletti, A. B. McDermott, J. W. Yewdell, J.

C. Sun, J. Chaudhuri, A hyper-IgM syndrome mutation in activation-induced cytidine deaminase disrupts G-quadruplex binding and genome-wide chromatin localization. *Immunity* **53**, 952–970.e11 (2020).

43. M. Ota, Y. Nagafuchi, H. Hatano, K. Ishigaki, C. Terao, Y. Takeshima, H. Yanaoka, S. Kobayashi, M. Okubo, H. Shirai, Y. Sugimori, J. Maeda, M. Nakano, S. Yamada, R. Yoshida, H. Tsuchiya, Y. Tsuchida, S. Akizuki, H. Yoshifuji, K. Ohmura, T. Mimori, K. Yoshida, D. Kurosaka, M. Okada, K. Setoguchi, H. Kaneko, N. Ban, N. Yabuki, K. Matsuki, H. Mutoh, S. Oyama, M. Okazaki, H. Tsunoda, Y. Iwasaki, S. Sumitomo, H. Shoda, Y. Kochi, Y. Okada, K. Yamamoto, T. Okamura, K. Fujio, Dynamic landscape of immune cell-specific gene regulation in immune-mediated diseases. *Cell* **184**, 3006–3021.e17 (2021).

44. A. Buniello, J. A. L. Macarthur, M. Cerezo, L. W. Harris, J. Hayhurst, C. Malangone, A. McMahon, J. Morales, E. Mountjoy, E. Sollis, D. Suveges, O. Vrousgou, P. L. Whetzel, R. Amode, J. A. Guillen, H. S. Riat, S. J. Trevanion, P. Hall, H. Junkins, P. Flicek, T. Burdett, L. A. Hindorff, F. Cunningham, H. Parkinson, The NHGRI-EBI GWAS Catalog of published genome-wide association studies, targeted arrays and summary statistics 2019. *Nucleic Acids Res.* **47**, D1005–D1012 (2019).

45. V. Orrù, M. Steri, C. Sidore, M. Marongiu, V. Serra, S. Olla, G. Sole, S. Lai, M. Dei, A. Mulas, F. Virdis, M. G. Piras, M. Lobina, M. Marongiu, M. Pitzalis, F. Deidda, A. Loizedda, S. Onano, M. Zoledziewska, S. Sawcer, M. Devoto, M. Gorospe, G. R. Abecasis, M. Floris, M. Pala, D. Schlessinger, E. Fiorillo, F. Cucca, Complex genetic signatures in immune cells underlie autoimmunity and inform therapy. *Nat. Genet.* **52**, 1036–1045 (2020).

46. C. Lin, E. R. Smith, H. Takahashi, K. C. Lai, S. Martin-Brown, L. Florens, M. P. Washburn, J. W. Conaway, R. C. Conaway, A. Shilatifard, AFF4, a component of the ELL/P-TEFb elongation complex and a shared subunit of MLL chimeras, can link transcription elongation to leukemia. *Mol. Cell.* **37**, 429–437 (2010).

47. J. N. Pucella, J. Chaudhuri, AID invited to the G4 summit. *Mol. Cell* **67**, 355–357 (2017).

48. Q. Qiao, L. Wang, F.-L. Meng, J. K. Hwang, F. W. Alt, H. Wu, AID recognizes structured DNA for class switch recombination. *Mol. Cell* **67**, 361–373.e4 (2017).

49. E. Pefanis, J. Wang, G. Rothschild, J. Lim, J. Chao, R. Rabadan, A. N. Economides, U. Basu, Noncoding RNA transcription targets AID to divergently transcribed loci in B cells. *Nature* **514**, 389–393 (2014).

50. U. Basu, F. L. Meng, C. Keim, V. Grinstein, E. Pefanis, J. Eccleston, T. Zhang, D. Myers, C. R. Wasserman, D. R. Wesemann, K. Januszyk, R. I. Gregory, H. Deng, C. D. Lima, F. W. Alt, The RNA exosome targets the AID cytidine deaminase to both strands of transcribed duplex DNA substrates. *Cell* **144**, 353–363 (2011).

51. R. Pavri, A. Gazumyan, M. Jankovic, M. Di Virgilio, I. Klein, C. Ansarah-Sobrinho, W. Resch, A. Yamane, B. R. San-Martin, V. Barreto, T. J. Nieland, D. E. Root, R. Casellas, M. C. Nussenzweig, Activation-induced cytidine deaminase targets DNA at sites of RNA polymerase II stalling by interaction with Spt5. *Cell* **143**, 122–133 (2010).

52. S. P. Methot, L. C. Litzler, P. G. Subramani, A. K. Eranki, H. Fifield, A.-M. Patenaude, J. C. Gilmore, G. E. Santiago, H. Bagci, J.-F. Côté, M. Larijani, R. E. Verdun, J. M. Di Noia, A licensing

step links AID to transcription elongation for mutagenesis in B cells. *Nat. Commun.* **9**, 1248 (2018).

53. K. L. Willmann, S. Milosevic, S. Pauklin, K. M. Schmitz, G. Rangam, M. T. Simon, S. Maslen, M. Skehel, I. Robert, V. Heyer, E. Schiavo, B. Reina-San-Martin, S. K. Petersen-Mahrt, A role for the RNA pol II-associated PAF complex in AID-induced immune diversification. *J. Exp. Med.* **209**, 2099–2111 (2012).

54. A.-S. Thomas-Claudepierre, E. Schiavo, V. Heyer, M. Fournier, A. Page, I. Robert, B. Reina-San-Martin, The cohesin complex regulates immunoglobulin class switch recombination. *J. Exp. Med.* **210**, 2495–2502 (2013).

55. M. Melko, D. Douguet, M. Bensaid, S. Zongaro, C. Verheggen, J. Gecz, B. Bardoni, Functional characterization of the AFF (AF4/FMR2) family of RNA binding proteins: Insights into the molecular pathology of FRAXE intellectual disability. *Hum. Mol. Genet.* **20**, 1873–1885 (2011).

56. N. A. Begum, A. Stanlie, M. Nakata, H. Akiyama, T. Honjo, The histone chaperone Spt6 is required for activation-induced cytidine deaminase target determination through H3K4me3 regulation. *J. Biol. Chem.* **287**, 32415–32429 (2012).

57. A. Stanlie, N. A. Begum, H. Akiyama, T. Honjo, The DSIF subunits Spt4 and Spt5 have distinct roles at various phases of immunoglobulin class switch recombination. *PLOS Genet.* **8**, e1002675 (2012).

58. I. M. Okazaki, K. Okawa, M. Kobayashi, K. Yoshikawa, S. Kawamoto, H. Nagaoka, R. Shinkura, Y. Kitawaki, H. Taniguchi, T. Natsume, S. I. Iemura, T. Honjo, Histone chaperone Spt6 is required

for class switch recombination but not somatic hypermutation. *Proc. Natl. Acad. Sci. U.S.A.* **108**, 7920–7925 (2011).

59. K. Izumi, R. Nakato, Z. Zhang, A. C. Edmondson, S. Noon, M. C. Dulik, R. Rajagopalan, C. P. Venditti, K. Gripp, J. Samanich, E. H. Zackai, M. A. Deardorff, D. Clark, J. L. Allen, D. Dorsett, Z. Misulovin, M. Komata, M. Bando, M. Kaur, Y. Katou, K. Shirahige, I. D. Krantz, Germline gain-of-function mutations in AFF4 cause a developmental syndrome functionally linking the super elongation complex and cohesin. *Nat. Genet.* **47**, 338–344 (2015).

60. A. Kim, L. Han, K. Yu, Immunoglobulin class switch recombination is initiated by rare cytosine deamination events at switch regions. *Mol. Cell. Biol.* **40**, e00125-20 (2020).

61. E. J. Wigton, Y. Mikami, R. J. McMonigle, C. A. Castellanos, A. K. Wade-Vallance, S. K. Zhou, R. Kageyama, A. Litterman, S. Roy, D. Kitamura, E. C. Dykhuizen, C. D. C. Allen, H. Hu, J. J. O'Shea, K. M. Ansel, MicroRNA-directed pathway discovery elucidates an miR-221/222–mediated regulatory circuit in class switch recombination. *J. Exp. Med.* **218**, e20201422 (2021).

62. R. Mandal, S. Becker, K. Strebhardt, Targeting CDK9 for anti-cancer therapeutics. *Cancers* **13**, 2181 (2021).

63. L. N. Almeida, A. Clauder, L. Meng, M. Ehlers, S. Arce, R. A. Manz, MHC haplotype and B cell autoimmunity: Correlation with pathogenic IgG autoantibody subclasses and Fc glycosylation patterns. *Eur. J. Immunol.* **52**, 197–203 (2022).

64. C. Vandamme, T. Kinnunen, B cell helper T cells and type 1 diabetes. *Scand. J. Immunol.* **92**, e12943 (2020).

65. C. M. Dayan, R. E. J. Besser, R. A. Oram, W. Hagopian, M. Vatish, O. Bendor-Samuel, M. D. Snape, J. A. Todd, Preventing type 1 diabetes in childhood. *Science* **373**, 506–510 (2021).

66. J. A. Bluestone, J. H. Buckner, K. C. Herold, Immunotherapy: Building a bridge to a cure for type 1 diabetes. *Science* **373**, 510–516 (2021).

67. K. Liang, E. R. Smith, Y. Aoi, K. L. Stoltz, H. Katagi, A. R. Woodfin, E. J. Rendleman, S. A. Marshall, D. C. Murray, L. Wang, P. A. Ozark, R. K. Mishra, R. Hashizume, G. E. Schiltz, A. Shilatifard, Targeting processive transcription elongation via SEC disruption for MYC-induced cancer therapy. *Cell* **175**, 766–779.e17 (2018).

68. C. A. Schneider, W. S. Rasband, K. W. Eliceiri, NIH Image to ImageJ: 25 years of image analysis. *Nat. Methods* **9**, 671–675 (2012).

69. S. Morita, T. Kojima, T. Kitamura, Plat-E: An efficient and stable system for transient packaging of retroviruses. *Gene Ther.* **7**, 1063–1066 (2000).

70. J. Xu, A. Husain, W. Hu, T. Honjo, M. Kobayashi, Ape1 is dispensable for S-region cleavage but required for its repair in class switch recombination. *Proc. Natl. Acad. Sci. U.S.A.* **111**, 17242–17247 (2014).

71. L. Lin, A. J. Gerth, S. L. Peng, CpG DNA redirects class-switching towards “Th1-like” Ig isotype production via TLR9 and MyD88. *Eur. J. Immunol.* **34**, 1483–1487 (2004).

72. N. S. Wang, L. J. McHeyzer-Williams, S. L. Okitsu, T. P. Burris, S. L. Reiner, M. G. McHeyzer-Williams, Divergent transcriptional programming of class-specific B cell memory by T-bet and RORα. *Nat. Immunol.* **13**, 604–611 (2012).

73. B. Reina-San-Martin, S. Difilippantonio, L. Hanitsch, R. F. Masilamani, A. Nussenzweig, M. C. Nussenzweig, H2AX is required for recombination between immunoglobulin switch regions but not for intra-switch region recombination or somatic hypermutation. *J. Exp. Med.* **197**, 1767–1778 (2003).

74. M. Dinkelmann, E. Spehalski, T. Stoneham, J. Buis, Y. Wu, J. M. Sekiguchi, D. O. Ferguson, Multiple functions of MRN in end-joining pathways during isotype class switching. *Nat. Struct. Mol. Biol.* **16**, 808–813 (2009).

75. R. C. Rickert, J. Roes, K. Rajewsky, B lymphocyte-specific, Cre-mediated mutagenesis in mice. *Nucleic Acids Res.* **25**, 1317–1318 (1997).

76. E. M. Cortizas, A. Zahn, M. E. Hajjar, A.-M. Patenaude, J. M. Di Noia, R. E. Verdun, Alternative end-joining and classical nonhomologous end-joining pathways repair different types of double-strand breaks during class-switch recombination. *J. Immunol.* **191**, 5751–5763 (2013).